Title

Enhanced fatigue endurance of metallic glasses through a staircase-like fracture mechanism

Journal

Proceedings of the National Academy of Sciences of the United States of America, 110(46)

ISSN

0027-8424

Authors

Gludovatz, Bernd
Demetriou, Marios D
Floyd, Michael
et al.

Publication Date

2013-11-12

DOI

10.1073/pnas.1317715110

Peer reviewed

Enhanced fatigue endurance of metallic glasses through a staircase-like fracture mechanism

Bernd Gludovatz[a], Marios D. Demetriou[b], Michael Floyd[b], Anton Hohenwarter[c], William L. Johnson[b,1], and Robert O. Ritchie[a,d,1]

[a]Materials Sciences Division, Lawrence Berkeley National Laboratory, Berkeley, CA 94720; [b]Keck Laboratory of Engineering Materials, California Institute of Technology, Pasadena, CA 91125; [c]Department of Materials Physics, University of Leoben, 8700 Leoben, Austria; and [d]Department of Materials Science and Engineering, University of California, Berkeley, CA 94720

Contributed by William L. Johnson, September 25, 2013 (sent for review December 28, 2012)

Bulk-metallic glasses (BMGs) are now candidate materials for structural applications due to their exceptional strength and toughness. However, their fatigue resistance can be poor and inconsistent, severely limiting their potential as reliable structural materials. As fatigue limits are invariably governed by the local arrest of microscopically small cracks at microstructural features, the lack of microstructure in monolithic glasses, often coupled with other factors, such as the ease of crack formation in shear bands or a high susceptibility to corrosion, can lead to low fatigue limits (some ∼1/20 of their tensile strengths) and highly variable fatigue lives. BMG-matrix composites can provide a solution here as their duplex microstructures can arrest shear bands at a second phase to prevent cracks from exceeding critical size; under these conditions, fatigue limits become comparable with those of crystalline alloys. Here, we report on a Pd-based glass that similarly has high fatigue resistance but without a second phase. This monolithic glass displays high intrinsic toughness from extensive shear-band proliferation with cavitation and cracking effectively obstructed. We find that this property can further promote fatigue resistance through extrinsic crack-tip shielding, a mechanism well known in crystalline metals but not previously reported in BMGs, whereby cyclically loaded cracks propagate in a highly "zig-zag" manner, creating a rough "staircase-like" profile. The resulting crack-surface contact (roughness-induced crack closure) elevates fatigue properties to those comparable to crystalline alloys, and the accompanying plasticity helps to reduce flaw sensitivity in the glass, thereby promoting structural reliability.

bulk amorphous alloy | fatigue life | damage tolerance

Since the late 1980s, multicomponent bulk-metallic glass (BMG) systems have developed into a class of materials with highly promising properties (1–3). High to ultrahigh strength (in some cases even greater than 5 GPa), in combination with low stiffness, high hardness, large elastic strain limits, and net-shape castability as well as good scratch and wear resistance, are among the main reasons making these materials potential candidates for many structural applications (4–11). However, as many BMGs are associated with near-zero tensile ductility and brittle fracture behavior, they can display low toughness as well as very low endurance (fatigue) limits in cyclic fatigue, all properties that are governed by the initiation and propagation of cracks. Indeed, many glasses fail catastrophically along a single shear band that evolves into a crack at vanishingly small tensile strains (12–15); this can lead to plane-strain fracture toughness K_{IC} values as low as ∼15–20 MPa$\sqrt{m}$ (16, 17).

As a consequence, high toughness in BMGs can be achieved by arresting propagating shear bands before cavitation can lead to a crack of critical size; shear-band arrest inevitably leads to multiple shear-band formation and as such provides a mechanism for extensive plastic flow and pronounced crack-tip blunting. This has been realized in glass-matrix composites by introducing a second phase in the form of crystalline dendrites and matching the microstructural size scales (i.e., the interdendritic spacing within the BMG matrix) to the mechanical size scales (i.e., the critical crack size) such that shear bands are arrested before they evolve into unstable cracks (18). By tailoring the volume fractions, interface strength, and elastic mismatch between the matrix and the second phase such that cracks intersect the dendrites, Zr-Ti-Nb-Cu-Be glass composites display K_{IC} values exceeding 150 MPa$\sqrt{m}$ with tensile strengths (σ_{UTS}) of 1.2–1.5 GPa. These composite glasses fail after subcritical crack growth, rather than by immediate catastrophic fracture, and hence show crack-resistance curve (R-curve) behavior with toughnesses as high as 200 MPa$\sqrt{m}$ (19). [The R-curve provides an assessment of the fracture toughness in the presence of subcritical cracking. It involves measurements of the crack-driving force, e.g., the linear-elastic stress intensity K, as a function of crack extension (Δa). The value of the driving force at $\Delta a \rightarrow 0$ is a measure of the crack-initiation toughness whereas the maximum value of the R-curve can be used to characterize the crack-growth toughness.] Furthermore, they have fatigue endurance strengths of ∼$0.3\sigma_{UTS}$ (20), i.e., comparable to polycrystalline structural alloys, suggesting that the composite approach provides one solution to the often low fatigue limits shown by BMGs, as monolithic glasses lack any microstructure that can provide means for the local arrest of incipient fatigue cracks.

Monolithic metallic glasses, in contrast, invariably display fatigue strengths that are far lower than those of polycrystalline structural metals, which clearly presents a problem as fatigue is the most common form of structural failure. For example, early ribbon metallic glasses displayed fatigue limits as low as $\sigma_a/\sigma_{UTS} \sim 0.05$ (21–23); similarly, initial studies on bulk metallic glasses such as Vitreloy 1 ($Zr_{41.25}Ti_{13.75}Ni_{10}Cu_{12.5}Be_{22.5}$) showed normalized 10^7-cycle endurance strengths of only $\sigma_a/\sigma_{UTS} \sim 0.04$ ($\sigma_a \sim 75$ MPa) (24, 25), although these values may have been influenced by

Significance

We believe this article is of broad interest to the materials science and engineering community. Bulk-metallic glasses (BMGs) are currently considered candidate materials for numerous structural applications. A major limitation in their use as engineering material is the often poor and inconsistent fatigue behavior. Although recently developed BMG composites provide one solution to this problem, fatigue remains a main issue for monolithic metallic glasses. The authors report unexpectedly high fatigue resistance in a monolithic Pd-based glass arising from extensive shear-band plasticity, resulting in a very rough and periodic "staircase" crack trajectory. The research both reveals a unique mechanism in fatigue of a monolithic metallic glass and demonstrates that this mechanism mitigates previous limitations on its use as an engineering material.

Author contributions: B.G., M.D.D., W.L.J., and R.O.R. designed research; B.G., M.D.D., M.F., and A.H. performed research; B.G., M.D.D., A.H., W.L.J., and R.O.R. analyzed data; and B.G., M.D.D., and R.O.R. wrote the paper.

The authors declare no conflict of interest.

[1]To whom correspondence may be addressed. E-mail: wlj@caltech.edu or roritchie@lbl.gov.

additional factors such as poor processing and environmental sensitivity (26). Subsequent improvements in the composition and processing techniques have led to higher fatigue limits in Zr-based glasses of $\sim 0.2\sigma_{UTS}$ (27, 28) or more (29, 30). Specifically, the compositional variant Vitreloy 105 ($Zr_{52.5}Ti_5Ni_{14.6}Cu_{17.9}Al_{10}$) is reported to exhibit a fatigue limit of $\sim 0.24\sigma_{UTS}$ (31, 32), but no specific mechanism responsible for such behavior is suggested either by the fracture morphology of this glass or by its overall fracture behavior. [Vitreloy 105 is far more brittle than the Pd glass, displaying lower toughness with no R-curve behavior, and as such is much more flaw sensitive. Stress-life (*S-N*) fatigue data accordingly tend to show considerable scatter; indeed, its endurance strength has been shown to be degraded by as much as 60% in the presence of casting porosity (32).] In general, due to a lack of plasticity, many monolithic glasses develop only very limited plastic zones at the tips of any incipient cracks, which can make these materials highly flaw sensitive; correspondingly, reported fatigue strengths often vary widely, such that comparisons must be taken with caution. Whereas it is clear that the microstructures of glass-matrix composites can locally arrest small cracks and thereby reliably show acceptable fatigue strengths, the question that remains is whether there are comparable mechanisms in monolithic glasses that can also generate such higher fatigue limits in a consistent and reliable manner comparable to that of polycrystalline structural metals ($\sim 0.3\sigma_{UTS}$).

To this end, we use here a newly developed monolithic Pd-based glass, which has been optimized for ultrahigh toughness, to discern whether any such fatigue endurance mechanisms exist. The amorphous alloy was developed to facilitate multiple shear band formation, thereby providing a mechanism for crack-tip blunting and high toughness (33). We show here that although there is no microstructure to hinder single shear-band formation or arrest small cracks, the fatigue threshold of this monolithic glass is 3.3 MPa$\sqrt{m}$ and the measured 10^7-cycle fatigue endurance strength approaches 0.24 σ_{UTS}, both properties that are among the highest for any monolithic glass and, in the case of the endurance strength, comparable to the best BMG composites and many traditional polycrystalline alloys. We demonstrate that this is achieved through a fatigue mechanism originating from the intrinsic capacity of this material to proliferate shear-band formation ahead of a crack tip to generate a "staircase-like" crack trajectory. This mechanism permits a significant degree of interlocking between mating crack surfaces, causing crack arrest via the well-known fatigue mechanism of roughness-induced crack closure (34), a mechanism that is not uncommon for polycrystalline materials but has not been reported previously for glasses.

Material Properties

The Pd-based monolithic glass studied, $Pd_{79}Ag_{3.5}P_6Si_{9.5}Ge_2$, was developed with high tensile strength ($\sim$1.5 GPa) and finite tensile ductility ($\sim$0.15%); it displays a glass-transition temperature T_g = 613 K, with respective bulk and shear moduli of B = 172 and G = 31 GPa and Poisson's ratio of $\sim$0.42 (33). It was reasoned that the large B/G ratio (with a high T_g) would make multiple shear-band formation ahead of a crack easier yet inhibit the cavitation processes that leads to fracture (35, 36). Indeed, this glass is among the most damage tolerant (strong and tough) of any metallic material reported to date (33), with extensive shear-band proliferation in micronotched three-point bend tests resulting in excessive crack-tip blunting and stable (subcritical) crack growth (R-curve behavior); fracture toughnesses as high as 200 MPa$\sqrt{m}$ (for crack extensions less than 500 μm) were measured for this glass, with no catastrophic fracture (33).

Cyclic Fatigue Resistance

Stress-life fatigue testing was performed to determine the *S-N* (Wöhler) curve and 10^7-cycle fatigue endurance strength for the amorphous $Pd_{79}Ag_{3.5}P_6Si_{9.5}Ge_2$ alloy. Results in the form of loading cycles to failure, N_f, as a function of the applied stress amplitude, σ_a (= $(\sigma_{max} - \sigma_{min})/2$), normalized by the (ultimate) tensile strength, σ_{UTS}, at a stress ratio R (= $\sigma_{min}/\sigma_{max}$) of 0.1 are shown in Fig. 1 and are compared with corresponding data for other monolithic and composite glasses. The normalized fatigue limit of the Pd-based glass, defined as the R = 0.1 endurance strength at 2×10^7 cycles, is $\sigma_a/\sigma_{UTS} \sim 0.24$, with an absolute value of σ_a = 360 MPa. Like most BMGs, this material contained pores and inclusions; provided they were smaller than 10 μm or so, the *S-N* data were unaffected, although an increased variability in lives was apparent at the higher stress levels. The mean endurance limit ($\sigma_a/\sigma_{UTS} \sim 0.24$) for the Pd-based glass is comparable to that of many polycrystalline metals and the best glass-matrix composites, specifically the DH3 alloy (matrix composition: $Zr_{34}Ti_{17}Nb_2Cu_9Be_{38}$), where $\sigma_a/\sigma_{UTS} \sim 0.3$ ($\sigma_a \sim 340$ MPa) (20); additionally, it is high compared with that of most other monolithic glasses (30).

Fatigue-crack growth thresholds (ΔK_{TH}) were also determined for the Pd glass by measuring growth rates (da/dN) as a function of the stress-intensity range, $\Delta K = K_{max} - K_{min}$ (where K_{min} is the minimum and K_{max} the maximum stress intensity). Values of ΔK_{TH} (at a load ratio $R = K_{min}/K_{max}$ of 0.1) were found to be 3.3 MPa$\sqrt{m}$, i.e., twice as high as that for Vitreloy 1, where $\Delta K_{TH} \sim 1.5$ MPa$\sqrt{m}$ (37), and 65% higher than the fatigue threshold of Vitreloy 105, where $\Delta K_{TH} \sim 2$ MPa$\sqrt{m}$ (32). As the fatigue properties of this monolithic Pd glass are comparable to those of the glass-matrix composite DH3, where the microstructure has been specifically tailored to stop shear-band cracks, the question that now remains is how such fatigue resistance is achieved in the absence of a microstructure to locally arrest such incipient flaws.

Mechanistic Aspects

With respect to mechanistic considerations, a vital characteristic of the Pd-based glass is its ability to undergo extensive plasticity but at high strength levels ($\sim$1.5 GPa) with limited cracking. This is in contrast to many BMGs where only minimal plastic flow in the vicinity of a flaw is possible, accommodated by limited nucleation and growth of a few shear bands. In the Pd glass, however, because of its much higher resistance to cavitation than to shear flow (33), such plasticity is extensive due to the excessive formation and proliferation of shear bands at a crack tip; moreover, these shear bands operate at high stress levels due to the generally high activation barriers, resulting from its high T_g (33). This can be seen in Fig. 2, which shows the nature of the deformation in the vicinity of a growing fatigue crack in a four-point bending test on this alloy. Regularly spaced shear-band patterns are seen ahead of the growing crack tip in the form of a fan-shaped Prandtl field (17, 23) extending across the whole ligament of the sample as well as in the crack wake. In an unnotched sample for the measurement of the fatigue endurance strength, such shear banding appears to form before crack initiation, which results in subsequent crack extension into a "sea" of shear bands, clearly resulting in pronounced crack-tip blunting (Fig. 2) and a lessened sensitivity to flaws.

Under cyclic loading, such blunting leads to the formation of fatigue striations, which represents the basic mechanism of fatigue-crack growth in ductile solids (38, 39). The striations form by a process of alternating crack-tip blunting on the loading cycle followed by resharpening on the unloading cycle; they are readily apparent on fatigue fracture surfaces in the present glass, as can be seen in Fig. 3. The extensive shear sliding within each band catalyzes the generation of secondary shear bands at nearly perpendicular orientations (i.e., at other maximum-resolved shear orientations), and as such, the propagation of the crack in this amorphous alloy occurs in a highly "zig-zag" manner preferentially along the surfaces of the primary and secondary shear bands, leaving a staircase-like crack surface (Fig. 4); as such, each

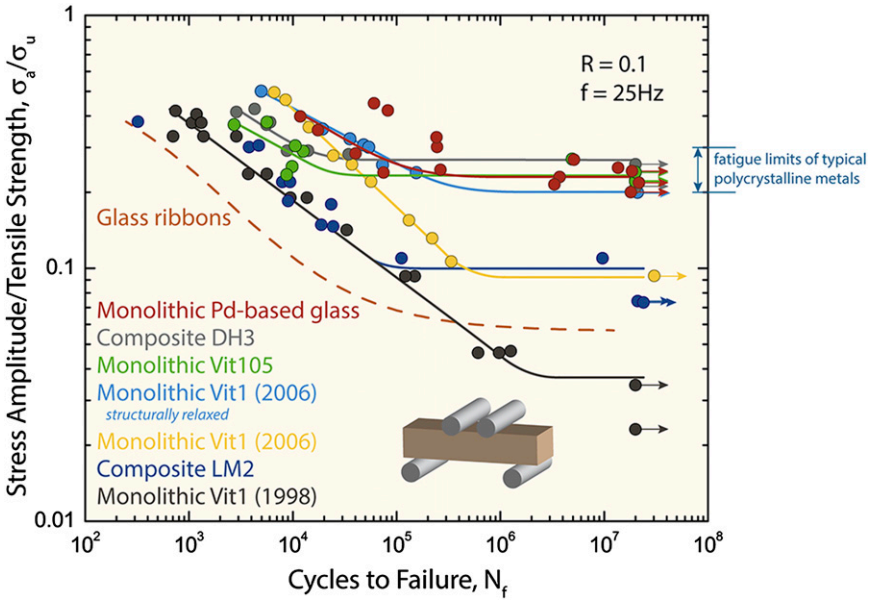

Fig. 1. Stress-life (*S-N*) fatigue data (*S-N*) of metallic glasses. *S-N* curves are presented in terms of the number of loading cycles, N_f, as a function of the applied stress amplitude, σ_a (= ($\sigma_{max} - \sigma_{min}$)/2), normalized by the ultimate tensile strength, σ_{UTS}, of the material. The fatigue limit of the Pd-based glass ($Pd_{79}Ag_{3.5}P_6Si_{9.5}Ge_2$), defined as the 2×10^7 cycles endurance strength at $R = 0.1$, is $\sigma_a/\sigma_{UTS} \sim 0.24$. The alloy has a high fatigue threshold ($\Delta K_{TH} \sim 3.3$ MPa$\sqrt{m}$) and achieves its fatigue resistance from the formation and proliferation of shear bands ahead of the crack tip, which causes significant crack-tip shielding. This leads to fatigue limits more than two times higher than those of LM2 ($Zr_{56.2}Ti_{13.8}Nb_5Cu_{6.9}Ni_{5.6}Be_{12.5}$) (28, 37), a BMG matrix composite, and up to four times higher than those of early monolithic ribbon metallic glasses (21–23); this is also above the endurance limit of the early monolithic glass Vitreloy 1 ($Zr_{41.25}Ti_{13.75}Ni_{10}Cu_{12.5}Be_{22.5}$), where normalized endurance limits of only $\sigma_a/\sigma_{UTS} \sim 0.04$ were measured (24, 25). Later versions of this alloy have shown normalized fatigue limits of $\sigma_a/\sigma_{UTS} \sim 0.09$ (27); further improvements in form of structural relaxation processes led to a decrease in the free volume of the glass and normalized endurance limits as high as $\sigma_a/\sigma_{UTS} \sim 0.2$ (27). The BMG composite DH3 ($Zr_{39.6}Ti_{33.9}Nb_{7.6}Cu_{6.4}Be_{12.5}$) represents the highest normalized fatigue limit, $\sigma_a/\sigma_{UTS} \sim 0.3$, of all metallic glasses (20) and the monolithic BMG Vitreloy 105 ($Zr_{52.5}Cu_{17.9}Ni_{14.6}Al_{10}Ti_5$) is plotted with its fatigue strength of $\sigma_a/\sigma_{UTS} \sim 0.25$ (31, 32). The regime of fatigue limits for typical polycrystalline metals is shown for comparison.

segment of the crack path resembles a local Forsyth's stage I crack (40). The crack path is continuous and deviates between shear bands with the highest shear stress; however, akin to Forsyth's stage II crack growth (40), it follows a global mode I crack path along a direction nominally perpendicular to the maximum tensile stresses. Nevertheless, the resulting crack surfaces remain significantly rough.

Many polycrystalline metals and alloys, especially planar-slip materials, show this particular fracture surface morphology (39, 41), but none to our knowledge are as pronounced as in this Pd-based glass. In polycrystalline alloys, such zig-zag crack paths are generally promoted by coarse grains, where the crack-tip plastic-zone size is less than the size of the grain diameter (34); as discussed below, this fracture surface morphology is highly beneficial to fatigue-crack resistance as it promotes crack-tip shielding from both crack deflection and more importantly asperity contact between the mating crack surfaces (34, 42, 43). What is particularly interesting and unexpected here is that such a tortuous crack path and the resulting highly faceted fracture can be achieved in an amorphous glass that essentially has no microstructure. This fatigue fracture mechanism is likely not unique in BMGs as most glasses show some degree of shear banding before cavitation; indeed there is one report of faceted fatigue fracture surface morphologies, in a $Zr_{50}Cu_{40}Al_{10}$ glass (44), but on a much smaller length scale than that of the current $Pd_{79}Ag_{3.5}P_6Si_{9.5}Ge_2$ glass.

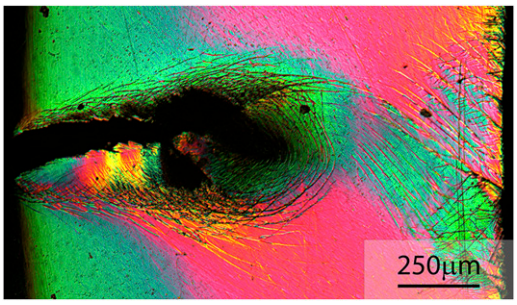

Fig. 2. Formation and proliferation of shear bands in the $Pd_{79}Ag_{3.5}P_6Si_{9.5}Ge_2$ amorphous alloy. Z-contrast optical micrograph shows pronounced formation and proliferation of shear bands throughout the thickness of a sample for a four-point bending stress life (*S-N*). The ability to form dense shear band networks is attributed to its high bulk-to-shear (*B/G*) modulus ratio (or equivalently, high Poisson's ratio) and its high glass-transition temperature (T_g). Such extensive shear banding ahead of a propagated fatigue crack occurs along fan-shaped (Prandtl-field) slip lines (17, 23) that bend from the tensile surface toward the compressive side of the sample and results in significant crack-tip blunting.

Discussion

Based on a comparison of the stress/life fatigue properties of a range of monolithic and composite bulk-metallic glass alloys, the monolithic Pd glass displays a very high (normalized) fatigue endurance limit of $\sigma_a/\sigma_{UTS} \sim 0.24$, consistent with its high fatigue threshold ($\Delta K_{TH} \sim 3.3$ MPa$\sqrt{m}$) and comparable to the best BMGs measured to date. We believe that such excellent fatigue behavior originates primarily from the ability of this glass to shield a propagating crack through excessive shear banding at the crack tip and the highly faceted staircase-like fracture surfaces (Fig. 4) that are generated as a consequence.

Cyclic loading at low stress ratios, e.g., at $R \sim 0.1$, invariably leads to some physical contact of the mating crack surfaces during the fatigue cycle. Such contact is well known as fatigue crack closure and has been reported for many crystalline materials (45);

ENGINEERING

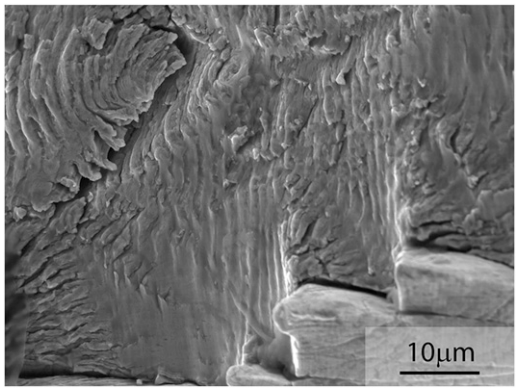

Fig. 3. Morphology of fatigue-crack propagation in the $Pd_{79}Ag_{3.5}P_6Si_{9.5}Ge_2$ amorphous alloy. SEM micrograph from the fracture surface of a stress-life (*S-N*) fatigue sample shows evidence of fatigue striations that result from the crack-tip blunting associated with extensive formation and proliferation of shear bands ahead of the crack tip. Crack propagation in fatigue occurs via a mechanism of alternating crack-tip blunting and resharpening, which leads to the formation of the striations.

as such, it represents a potent mechanism of extrinsic toughening (41) that effectively raises the minimum stress intensity $K_{\min}$ in the cycle, thereby reducing the effective ΔK range actually experienced at the crack tip (crack-tip shielding). [Fracture can be considered as a mutual competition between intrinsic and extrinsic toughening mechanisms. Intrinsic toughening mechanisms operate ahead of the crack tip to generate resistance to microstructural damage, the most prominent of which is plastic deformation that provides a means of blunting the crack tip through the formation of plastic zones. Extrinsic toughening mechanisms, conversely, operate primarily in the wake of the crack tip to inhibit the growth of a crack by "shielding" it from the applied driving force (41). Whereas intrinsic toughening is effective in inhibiting both the initiation and growth of cracks, extrinsic mechanisms, e.g., crack closure, are effective only in inhibiting crack growth.] With rough fracture surfaces in the presence of some degree of crack-tip shear displacements in metallic materials, this contact can result from corrosion debris on the crack surfaces (oxide-induced crack closure) or more generally from rough fracture surfaces that promote asperity wedging between mating crack surfaces (roughness-induced crack closure) (34, 42, 43). This creates a crack-tip shielding effect that is maximized when the stresses (or stress intensities) are low, because this is where the crack-tip opening displacements (CTODs) are smallest and hence are comparable with the size of the crack surface wedge; this is achieved close to the endurance strength or fatigue threshold.

The propensity for multiple shear-band formation and the resulting pronounced zig-zag crack surface in the current Pd-based glass (Fig. 4) acts to enhance the fatigue resistance in several ways. For a start, the deflection of the crack trajectory from the plane of maximum tensile stress acts to reduce the stress intensity actually experienced at the crack tip. For a roughly 45° deflection (in-plane kink) of the crack path, as shown in Fig. 4, simple crack deflection mechanics (46) suggest a reduction in the local crack-tip stress intensity on the order of 15%. However, more importantly, the highly serrated crack surfaces can interact and disrupt the opening and closing of the crack during the fatigue cycle. As can be seen in the scanning electron micrograph in Fig. 5, these crack surfaces resemble interlocking gear teeth, with asperities some 50 μm in height, forming in the wake of cracks as small as 1 mm or so. This represents a truly extreme form of roughness-induced crack closure, and the consequent shielding undoubtedly reduces the driving force actually experienced at the crack tip for continued crack growth, thus providing the primary mechanism for the local arrest of incipient cracks.

Estimates of the quantitative magnitude of this shielding effect can be obtained using simple 2D geometric models of this phenomenon (39). The Suresh and Ritchie model of roughness-induced closure suggests that the magnitude of the shielding depends upon the size of crack-surface asperities and the extent of crack-tip shear displacements. Specifically, the closure stress intensity K_{cl} at the point of first asperity contact is given in terms of the maximum stress intensity K_{max} as (39)

$$K_{cl} \sim \sqrt{\frac{2\gamma u}{1+2\gamma u}}\, K_{max}, \qquad [1]$$

where γ is a measure of surface roughness (ratio of height to width of the asperities), and u is the ratio of mode II to mode I displacements. For the Pd-based glass alloy, values of γ from the crack-path profile in Fig. 5 can be used to approach values of ~0.5. Using Eq. **1**, this implies that very significant levels of crack closure, i.e., up to a 50% reduction in the effective stress intensity, can arise for shear displacements of only 30% of the mode I crack opening. Because the fatigue lifetimes in metallic materials at these low stress intensities (or stresses) tend to scale with the reciprocal of the stress intensity (or stress) raised to some high power, generally between 2 and 10, a factor of 2 reduction in the stress intensity experienced at the crack tip would translate into a very significant increase in fatigue life and likely arrest the growing crack.

As noted, this staircase-like fracture mechanism in such an extreme form has never been identified previously in fatigue of any BMGs most likely due to the more brittle nature of many monolithic glasses and thus less pronounced shear banding at the crack tip occurring over much shorter length scales. It is indeed remarkable that such a rough, highly faceted fracture associated with such large length scales can occur in a glass. Its effect, however, which is clearly promoted where excessive multiple shear banding can occur, certainly results in very significant crack-tip shielding, which can act to suppress or delay the growth of small cracks from preexisting flaws. The effect is multifold: The formation of shear bands leads to extensive crack-tip blunting (by plastic deformation leading to intrinsic toughening), which also

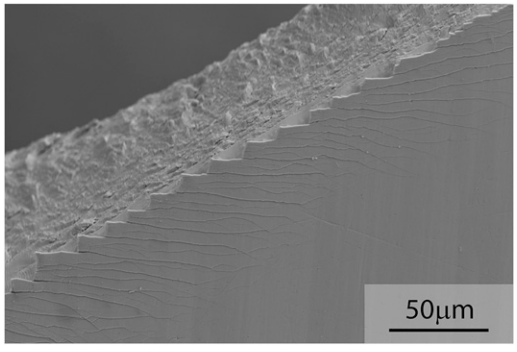

Fig. 4. Scanning electron microscope (SEM) image of the crack wake of $Pd_{79}Ag_{3.5}P_6Si_{9.5}Ge_2$. Global crack propagation occurs from the crack initiation site on the tensile surface of the sample (upper right) toward the compressive side of the sample (lower left) whereas local deviations in the crack propagation direction lead to a "staircase-like" crack path and a rough fracture surface. The "stairs" are associated with lengths scales on the order of 5–50 μm, depending upon the local stress intensities and the orientation of the crack. Deviations in the crack path are a result of a locally decreased crack propagation resistance along slip planes of shear bands.

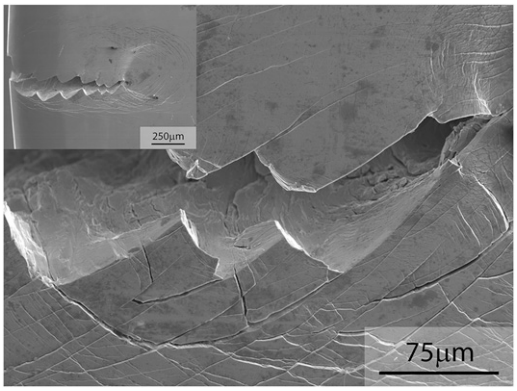

Fig. 5. Crack tip and immediate wake of a growing fatigue crack in the $Pd_{79}Ag_{3.5}P_6Si_{9.5}Ge_2$ monolithic glass. *Inset* of the SEM image shows excessive formation and proliferation of shear bands from the crack tip of a propagating fatigue crack during an *S-N* test. Crack propagation occurs along the slip planes of primary shear bands, leading to a highly deviated crack path revealing "stairs", in this instance with lengths scales on the order of 50 μm. The irreversible nature of inelastic crack-tip displacement leads to crack-asperity wedging on unloading as a result of physical contact of the mating crack surfaces during cyclic crack growth. This results in an elevation in the effective value of K_{min}, which acts to significantly reduce the applied ΔK range actually experienced at the crack. Such pronounced contact shielding of the crack tip, termed roughness-induced crack closure, is most effective at low load ratios and small cyclic crack-tip open displacements (ΔCTODs), where the size of the crack asperities becomes comparable to that of ΔCTOD (41). The shielding is particularly pronounced in the current Pd glass due to the occurrence of significant crack-tip shear displacements as well as frequent crack deflections, as shown in the SEM image.

reduces the flaw sensitivity of the glass, whereas resulting crack deflection and crack closure act to inhibit crack growth (by crack-tip shielding leading to extrinsic toughening). These mechanisms, together with the high fatigue threshold, clearly provide the major contributions to the excellent fatigue endurance strength shown by the Pd-based glass.

Closure

In this work on a Pd-based glass, we have shown that excessive shear band formation, with limited cavitation, not only promotes exceptional strength and toughness, but also further imparts excellent fatigue resistance due to enhanced crack-tip shielding associated with highly serrated crack paths along these bands. The development of the often mutually exclusive properties of strength and toughness is in itself a significant challenge (47); further combining this with excellent fatigue resistance in many respects represents an ideal suite of properties for a structural material.

Methods

Materials Processing. $Pd_{79}Ag_{3.5}P_6Si_{9.5}Ge_2$ alloys were prepared by melting pure elements inductively in quartz tubes under inert atmosphere. Alloy ingots were fluxed with B_2O_3 at ~1,200 K for ~1,000 s. Amorphous rods, 3 mm in diameter, were produced by melting the fluxed ingots in quartz tubes with 0.5-mm-thick walls and rapidly water quenching. The amorphous structures of the specimens were verified by X-ray diffraction. Samples for mechanical testing were machined directly from these ingots.

Characterization. Samples were mechanically polished to a 1-μm diamond suspension surface finish. To investigate the mechanistic origins of the initiation of fatigue cracking as well as the failure mechanism during early propagation, structures and fracture surfaces were investigated using an interference contrast technique on a Zeiss Axiotech 100 reflected-light microscope (Carl Zeiss MicroImaging) and using a scanning electron microscopy (SEM) Hitachi S-4300SE/N ESEM (Hitachi America) operated at a vacuum of 10^{-4} Pa and 20 kV excitation voltage in secondary electron mode.

***S-N* Experiments.** Rectangular unnotched beams, with thickness $B \sim 2$ mm and width $W \sim 2$ mm, were cycled in four-point bending (tension–tension loading), using an inner loading span, $S_1 > 2W$, and an outer span, $S_2 > 4W$. Samples were polished with diamond paste to a 1-μm finish on the tensile surface and the corners were slightly rounded to reduce any stress concentration. Tests were performed in air, using a servo-hydraulic MTS 810 mechanical testing machine (MTS Corporation). Loads were applied under load control at a frequency of 25 Hz (sine wave) and a constant load (or stress) ratio of $R = 0.1$ (ratio of minimum to maximum load). Stresses σ at the tensile surface within the inner span were calculated using simple beam mechanics theory in terms of the applied load P:

$$\sigma = \frac{3P(S_2 - S_1)}{2BW^2}. \quad [2]$$

Beams were tested between $\sigma_a/\sigma_{UTS} \sim 0.20$–$0.45$, where σ_a, the applied stress amplitude, is normalized by the ultimate tensile strength, σ_{UTS}, of the material. σ_a is defined as half of the stress range, $\Delta\sigma$, and $\Delta\sigma = \sigma_{min} - \sigma_{max}$, where σ_{min} and σ_{max} correspond, respectively, to the minimum and maximum values of the applied stress. Tests were terminated in cases where failure had not occurred after 2×10^7 cycles (~9 d at 25 Hz). Data are presented in the form of *S-N* curves, where the number of cycles to failure, N_f, is plotted as a function of the applied normalized stress amplitude, σ_a/σ_{UTS}, as shown in Fig. 1.

Fatigue-Threshold Tests. Twelve-millimeter-long beam-like samples, of width $W \sim 2$ mm with thickness $B \sim 2$ mm, were mechanically polished to a 1-μm surface finish. A rounded notch was introduced using a diamond blade, sharpened using a razor blade irrigated in 1 μm diamond suspension, and then precracked by fatigue under cyclic compression–compression loading ($\Delta K \sim 5$–6 MPa$\sqrt{m}$, $R \sim 20$), using a Rumul Mikrotron 654 testing machine to an *a/W* of ~0.2. The fatigue threshold was measured by cycling the beams in three-point bending (tension–tension loading at $R = 0.1$) in an automated servo-electric MTS Tytron 250 testing machine at a sinusoidal frequency of 25 Hz under load control. Samples were initially cycled for $\sim 10^5$ cycles at ΔK levels below the expected threshold, before crack propagation was checked using an optical microscope (Olympus BX 51). If no crack propagation was observed, ΔK was increased with an increment of ~0.2 MPa$\sqrt{m}$. Once crack propagation occurred, it was additionally verified using a LEO (Zeiss) 1525 FE-SEM (Carl Zeiss), operating at 20 kV in secondary electron mode.

ACKNOWLEDGMENTS. This work was funded by the Director, Office of Science, Office of Basic Energy Sciences, Division of Materials Sciences and Engineering, of the US Department of Energy under Contract DE-AC02-05CH11231 (which provided financial support for B.G. and R.O.R.). M.D.D., M.F., and W.L.J. acknowledge funding support from the Office of Naval Research under Contract N00014-07-1-1115.

1. Byrne CJ, Eldrup M (2008) Materials science. Bulk metallic glasses. *Science* 321(5888): 502–503.
2. Inoue A, Yamaguchi H, Zhang T, Masumoto T (1990) Al-La-Cu amorphous alloys with a wide supercooled liquid region. *Mater Trans JIM* 31(2):104–109.
3. Inoue A, Zhang T, Masumoto T (1989) Al-La-Ni amorphous alloys with a wide supercooled liquid region. *Mater Trans JIM* 30(12):965–972.
4. Inoue A (2000) Stabilization of metallic supercooled liquid and bulk amorphous alloys. *Acta Mater* 48(1):279–306.
5. Löffler JF (2003) Bulk metallic glasses. *Intermetallics* 11(6):529–540.
6. Inoue A, Shen B, Takeuchi A (2006) Developments and applications of bulk glassy alloys in late transition metal base system. *Mater Trans JIM* 47(5):1275–1285.
7. Peter W, et al. (2002) Localized corrosion behavior of a zirconium-based bulk metallic glass relative to its crystalline state. *Intermetallics* 10(11-12):1157–1162.
8. Morrison ML, et al. (2005) The electrochemical evaluation of a Zr-based bulk metallic glass in a phosphate-buffered saline electrolyte. *J Biomed Mater Res A* 74(3):430–438.
9. Liaw PK, Miller MK, eds (2008) *Bulk Metallic Glasses: An Overview* (Springer, New York).
10. Schroers J (2005) The superplastic forming of bulk metallic glasses. *JOM* 57(5):35–39.
11. Ashby MF, Greer AL (2006) Metallic glasses as structural materials. *Scr Mater* 54(3): 321–326.
12. Pampillo CA (1972) Localized shear deformation in a glassy metal. *Scr Metall* 6(10):915–917.
13. Schuh CA, Hufnagel TC, Ramamurty U (2007) Mechanical behavior of amorphous alloys. *Acta Mater* 55(12):4067–4109.
14. Bruck HA, Christman T, Rosakis AJ, Johnson WL (1994) Quasi-static constitutive behavior of Zr41.25Ti13.75Ni10Cu12.5Be22.5 bulk amorphous alloys. *Scr Metall Mater* 30(4):429–434.

15. Flores KM, Dauskardt RH (2001) Mean stress effects on flow localization and failure in a bulk metallic glass. *Acta Mater* 49(13):2527–2537.
16. Lowhaphandu P, Lewandowski JJ (1998) Fracture toughness and notched toughness of bulk amorphous alloy: Zr-Ti-Ni-Cu-Be. *Scr Mater* 38(12):1811–1817.
17. Flores KM, Dauskardt RH (1999) Enhanced toughness due to stable crack tip damage zones in bulk metallic glass. *Scr Mater* 41(9):937–943.
18. Hofmann DC, et al. (2008) Designing metallic glass matrix composites with high toughness and tensile ductility. *Nature* 451(7182):1085–1089.
19. Launey ME, et al. (2009) Fracture toughness and crack-resistance curve behavior in metallic glass-matrix composites. *Appl Phys Lett* 94(24):241910.
20. Launey ME, Hofmann DC, Johnson WL, Ritchie RO (2009) Solution to the problem of the poor cyclic fatigue resistance of bulk metallic glasses. *Proc Natl Acad Sci USA* 106(13):4986–4991.
21. Ogura T, Masumoto T, Fukushima K (1975) Fatigue fracture of amorphous Pd-20at.% Si alloy. *Scr Metall* 9(2):109–113.
22. Davis LA (1976) Fatigue of metallic glasses. *J Mater Sci* 11(4):711–717.
23. Alpas A, Edwards L, Reid C (1989) Fracture and fatigue crack propagation in a nickel-base metallic glass. *Metall Mater Trans A* 20(8):1395–1409.
24. Gilbert CJ, Lippmann JM, Ritchie RO (1998) Fatigue of a Zr-Ti-Cu-Ni-Be bulk amorphous metal: Stress/life and crack-growth behavior. *Scr Mater* 38(4):537–542.
25. Menzel BC, Dauskardt RH (2006) Stress-life fatigue behavior of a Zr-based bulk metallic glass. *Acta Mater* 54(4):935–943.
26. Philo SL, Kruzic JJ (2010) Fatigue crack growth behavior of a Zr–Ti–Cu–Ni–Be bulk metallic glass: Role of ambient air environment. *Scr Mater* 62(7):473–476.
27. Launey ME, Busch R, Kruzic JJ (2006) Influence of structural relaxation on the fatigue behavior of a Zr41.25Ti13.75Ni10Cu12.5Be22.5 bulk amorphous alloy. *Scr Mater* 54(3):483–487.
28. Wang GY, et al. (2006) Comparison of fatigue behavior of a bulk metallic glass and its composite. *Intermetallics* 14(8-9):1091–1097.
29. Wang GY, Liaw PK, Yokoyama Y, Inoue A, Liu CT (2008) Fatigue behavior of Zr-based bulk-metallic glasses. *Mater Sci Eng A Struct Mater* 494(1-2):314–323.
30. Wang GY, Liaw PK, Morrison ML (2009) Progress in studying the fatigue behavior of Zr-based bulk-metallic glasses and their composites. *Intermetallics* 17(8):579–590.
31. Morrison ML, et al. (2007) Four-point-bending-fatigue behavior of the Zr-based Vitreloy 105 bulk metallic glass. *Mater Sci Eng A Struct Mater* 467(1-2):190–197.
32. Naleway SE, Greene RB, Gludovatz B, Dave NKN, Ritchie RO (2013) A highly fatigue resistant Zr-based bulk metallic glass. *Metall Mater Trans A*, in press.
33. Demetriou MD, et al. (2011) A damage-tolerant glass. *Nat Mater* 10(2):123–128.
34. Suresh S, Ritchie RO (1982) A geometric model for fatigue crack closure induced by fracture surface roughness. *Metall Mater Trans A* 13(9):1627–1631.
35. Lewandowski JJ, Wang WH, Greer AL (2005) Intrinsic plasticity or brittleness of metallic glasses. *Philos Mag Lett* 85(2):77–87.
36. Schroers J, Johnson WL (2004) Ductile bulk metallic glass. *Phys Rev Lett* 93(25):255506.
37. Flores KM, Johnson WL, Dauskardt RH (2003) Fracture and fatigue behavior of a Zr–Ti–Nb ductile phase reinforced bulk metallic glass matrix composite. *Scr Mater* 49(12): 1181–1187.
38. Laird C (1967) The influence of metallurgical structure on the mechanisms of fatigue crack propagation. *Fatigue Crack Propagation*, ASTM Special Technical Publication 415, ed Grosskreutz J (American Society for Testing and Materials, Philadelphia), pp 131–168.
39. Neumann P (1969) Coarse slip model of fatigue. *Acta Metall* 17(9):1219–1225.
40. Forsyth PJE (1962) A two stage process of fatigue crack growth. *Crack Propagation: Proceedings of Cranfield Symposium* (Her Majesty's Stationery Office, London), Vol 1, pp 76–94.
41. Ritchie RO (1988) Mechanisms of fatigue crack propagation in metals, ceramics and composites: Role of crack tip shielding. *Mater Sci Eng A Struct Mater* 103(1):15–28.
42. Walker N, Beevers CJ (1979) A fatigue crack closure mechanism in titanium. *Fatigue Fracture Eng Mater Struct* 1(1):135–148.
43. Minakawa K, McEvily AJ (1981) On crack closure in the near-threshold region. *Scr Metall* 15(6):633–636.
44. Wang G, et al. (2010) Fatigue initiation and propagation behavior in bulk-metallic glasses under a bending load. *J Appl Phys* 108(11):113512.
45. Elber W (1970) Fatigue crack closure under cyclic tension. *Eng Fract Mech* 2(1):37–45.
46. Cotterell B, Rice JR (1980) Slightly curved or kinked cracks. *Int J Fract* 16(2):155–169.
47. Ritchie RO (2011) The conflicts between strength and toughness. *Nat Mater* 10(11): 817–822.